



# Synthesis, Characterization, and Dye Removal Applications of Graphene Oxide-Gold Nanocomposite

Somayeh Sadighian<sup>1,\*</sup> , Manijeh Tozihi<sup>2</sup> 

<sup>1</sup> Department of Pharmaceutical Biomaterials, School of Pharmacy, Zanjan University of Medical Sciences, Zanjan, Iran

<sup>2</sup> Department of Chemistry, University of Zanjan, Zanjan, Iran

\* Correspondence: [somayeh.sadighian@gmail.com](mailto:somayeh.sadighian@gmail.com) (S.S.);

Scopus Author ID: 26325122200

Received: 15.07.2022; Accepted: 26.08.2022; Published: 31.10.2022

**Abstract:** Here, we report the facile synthesis of graphene oxide/gold nanocomposite, and dye removal ability as an adsorbent was studied. Sodium citrate as a reducing agent was used to reduce Au (III) ions to the formation of gold nanoparticles on the surface of graphene oxide sheets that were prepared by Hummers' method. Transmission electron microscopy (TEM), Fourier transform infrared spectroscopy (FT-IR), and X-ray diffraction (XRD) was used to specify nanocomposite synthesis. Adsorption dosage and contact time were investigated and explained as influencing parameters in removing methylene blue and methyl orange. In optimum conditions, the amount of adsorbent 30 mg and contact time 15 min for methylene blue and the amount of adsorbent 30 mg and contact time 25 min for methyl orange were quantitatively removed from 10 mL of wastewater. The pseudo-second-order model explained the kinetic data. Since graphene oxide/gold nanocomposite could be reused reasonably and had adsorptive properties, it tends to be produced as a modest and elective adsorbent to treat wastewater.

**Keywords:** synthesis; graphene oxide/gold nanocomposite; methyl orange; dye; kinetic.

© 2022 by the authors. This article is an open-access article distributed under the terms and conditions of the Creative Commons Attribution (CC BY) license (<https://creativecommons.org/licenses/by/4.0/>).

## 1. Introduction

Currently, the drinking water supply has become one of the problems of human society because of the lack of water resources [1-3]. Water is important for preserving living organisms, and water pollution has become a global problem. One of the most dangerous water pollutants, even small amounts, are dyes and aromatic [4,5]. The use of aromatic dyes and other pollutants has enhanced globally since the industrial revolution [6]. Various methods have been used to remove contaminants from water, such as membrane filtration, optical decomposition, and reverse osmosis [7].

Nevertheless, some of these methods have limitations, such as cost and complexity. The adsorption method is one of the simplest and best systems for this purpose and does not cause secondary contamination [8]. After adsorbing contaminants from water, the adsorbent can be recycled and reused. Researchers are constantly researching to improve the quality of adsorbents. A successful adsorbent should have a high adsorption rate and capacity and be selective [9,10]. Porous materials, metal-organic frameworks, activated carbon, etc., have been used as adsorbents to achieve this goal. Among these, carbon-based materials are more important as a result of their high adsorption capacity [11,12].

Graphene oxide (GO) is a 2D nanomaterial with  $sp^2$  hybridization that has functional groups of epoxide, hydroxyl, and carboxylic acid on its surface. Because of its great surface

area has been considered in many water treatment methods [13,14]. Metal nanoparticles are also used for decolorization. The size and shape of nanoparticles play an important role in this regard, and different synthesis methods can be used to prepare different shapes of these nanoparticles. One of the nanoparticles' high tendency to aggregate reduces their performance. Hence, methods such as blending with polymers or coating with other materials are used to prevent irreversible aggregation. Another method is to use graphene oxide as a substrate. Metal nanoparticles act as a spacer inside the graphene oxide sheets and prevent agglomeration during the reduction process [15]. Adsorption of the dye into graphene oxide is due to hydrogen bonding and  $\pi$ - $\pi$  interaction [16,17]. Graphene oxide adsorbs anionic less than cationic dyes due to its strong electrostatic repulsion with them [18].

In this study, methyl orange (MO) dye was used, an azo and industrial dye. It is used in the industry because of its low cost and high effectiveness. Also, methylene blue (MB) was used as cationic dye material that was utilized in wool, silk, and cotton products. Although MO and MB are not dangerous, prolonged exposure can increase heart rate, shock, jaundice, vomiting, etc. Thus, the removal of these two from the wastewater was significant and was chosen as model dyes [19,20].

In this research, GO-Au nanocomposites are synthesized with the appropriate surface area by an easy method without any additional treatment. Then, synthesized nanocomposite adsorption behavior studies for water treatment.

## 2. Materials and Methods

### 2.1. Materials and reagents.

Graphite, Hydrogen tetrachloroaurate (III) ( $\text{HAuCl}_4 \cdot 4\text{H}_2\text{O}$ ), sodium hydroxide (NaOH), potassium permanganate ( $\text{KMnO}_4$ ), polysorbate 80 (TWEEN 80), hydrogen peroxide, methyl orange (MO), methylene blue (MB), hydrochloric acid, and sulfuric acid were purchased locally from Merck and used as received. Chitosan  $10^5 - 3 \times 10^5$  g/mol and degree of deacetylation  $\geq 75\%$  provided by Sigma.

### 2.2. Synthesis of GO.

GO was made through the Hummers method with the usage of graphite powder. In a common synthesis, 0.5 g of graphite and  $\text{H}_2\text{SO}_4$  (24 mL) were agitated at ambient temperature for about 2 h. Next, the combination was kept at a low temperature, and  $\text{KMnO}_4$  (1.2 g) was gently added to the mixture. Next, the mixture was heated to 30–35 °C and stirred for the other 24 h. Afterward, 20 mL of deionized water was added to the mixture for 5 min. To end, 10 mL of distilled water and 5 mL of 30%  $\text{H}_2\text{O}_2$  were added to the mix to finish the reaction. In the final step, the resultant mixture was washed with  $\text{H}_2\text{O}$  and 5% HCl till the pH achieved 5–6 and dried. Eventually, GO was synthesized [21,22].

### 2.3. Preparation of GO-Au nanocomposite.

A 20 mg of graphene oxide concentration in 10 mL of distilled water was dispersed and sonicated by a two-hour ultrasonic bath. 20 mg of graphene oxide in 10 mL of distilled water was dispersed and sonicated for 2 h. Next, 5 mL of 8 mM  $\text{HAuCl}_4$ , 1 mL chitosan solution (0.5% (w/v) in acetate buffer (pH= 4.8)), and 100  $\mu\text{L}$  of 1 M NaOH aqueous solution were added to

the GO dispersion by gently shaking. The final product was washed in deionized water and dried at ambient temperature [23].

#### 2.4. Adsorption experiments.

MO and MB adsorption in water-based solutions through GO-Au nanocomposite was discussed. The adsorption amount of colorant factor by nanocomposite was determined by adding a variety of adsorbent/dye concentrations. After the speed of 100 rpm stirring for 30 min at  $25 \pm 1^\circ\text{C}$ , the suspension was centrifuged, and a trace of the supernatant was collected for assessment. The concentration of MO and MB in the supernatant was investigated using a UV-Vis spectrophotometer at  $\lambda_{\text{max}} = 465$  nm and 660, sequence.  $Q_t$ , the quantity of adsorbed dye was calculated by Equation (1):

$$q_t = \frac{(C_0 - C) V}{W} \quad (1)$$

$$E = \frac{(C_0 - C)}{C_0} \times 100\% \quad (2)$$

where,  $C_0$  (mg/L) and  $C$  (mg/L) are the primary and the equilibrium concentrations of dyes in the solution,  $V$  (L) is the total volume of the solution, and  $W$  (g) is the weight of the adsorbent.

#### 2.5. Characterization of the synthesized nanocomposite.

The crystallinity of the structural samples was examined using a Bruker D8 Advance diffractometer with Cu- $K_\alpha$  radiation ( $\lambda = 1.54 \text{ \AA}$ ). A UV-Vis spectrometer (Genesys, Madison, WI, USA) with 1 cm quartz cells has been used to determine UV-Vis absorbance spectra. Fourier-transform infrared (FT-IR) spectra were done on a Bruker Tensor 27 (Biotage, Germany) using pressed KBr disks. Transmission electron microscopy (TEM) has been used to study nanocomposite size and morphology (CM120 TEM (Philips)).

#### 2.6. Reusability test.

Moreover, to the dye elimination activity, stability is an additional important factor in specifying the usage of the catalysts in applications [24]. The adsorbent regeneration was done by desorption of dye from the GO-Au nanocomposite. Desorption of dye molecules was performed by using 100 mg adsorbent in 500 ml of 0.1 M NaOH solution for 24 hours. Afterward, shaken at 5000 rpm and  $24 \pm 1^\circ\text{C}$ , the nanocomposite was removed and dried at a temperature of  $60^\circ\text{C}$  for 24 hours.

### 3. Results and Discussions

#### 3.1. Characterization of the nanocomposite.

##### 3.1.1. XRD analysis.

XRD patterns of GO-Au nanocomposite are shown in Figure 1. The crystal structure of the graphene oxide has been verified at  $2\theta = 11.4^\circ$  corresponding to the (001). The diffraction peak at  $21^\circ$  demonstrates the (001) crystal face of graphene oxide, suggesting that the regular GO sheets were destroyed by the interaction of Au NPs with the GO surface, which is similar to as described in our previous article [23].

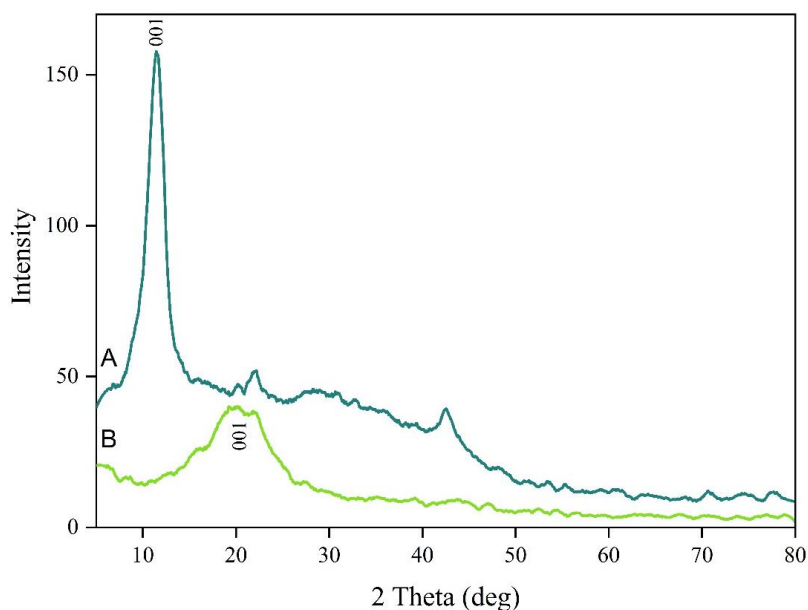


**Figure 1.** XRD patterns of the (A) GO and (B) GO-Au nanocomposite.

### 3.1.2. Fourier-transform infrared spectroscopy analysis.

FT-IR spectra of the GO and GO-Au nanocomposite are displayed in Figure 2. The  $1084\text{ cm}^{-1}$  peak is correlated with the C-O bond. The peak at  $1631$  and  $1735\text{ cm}^{-1}$  can be set to the vibrations of aromatic C=C in graphene rings and stretching of the C=O and COOH groups on GO sheets, respectively. The band at  $3434\text{ cm}^{-1}$  shows the O-H stretching bond. The FT-IR spectra of GO-Au nanocomposite are demonstrated (Figure 2b). The bands at  $1090$  and  $1588\text{ cm}^{-1}$  showed chitosan C-N and N-H groups, respectively [25], matching the creation of GO-Au nanocomposite. Besides, the new band at  $3200\text{ cm}^{-1}$  appears to have an N-H stretching vibration, confirming the deposition of Au NPs with a chitosan shell.

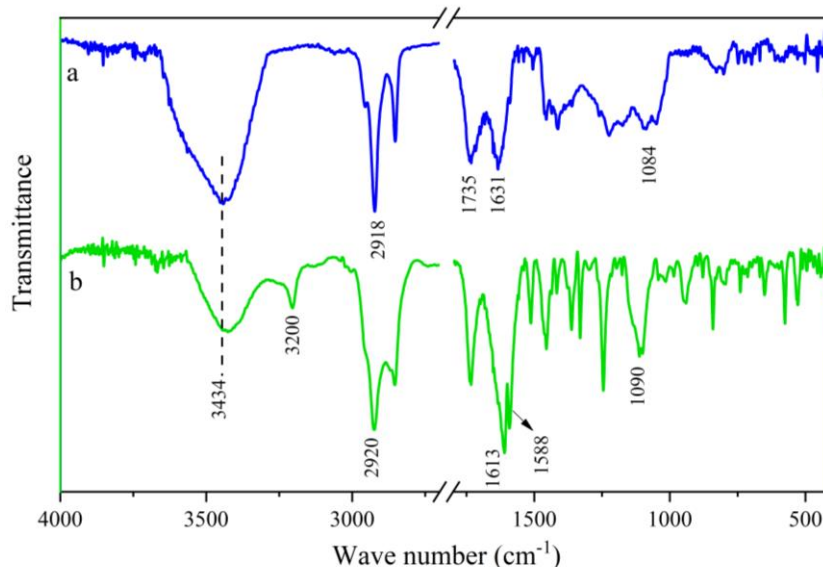


**Figure 2.** FT-IR Spectra of (a) GO and (b) GO-Au nanocomposite.

### 3.1.3. Morphological characterization.

Figure 3 demonstrates a TEM image of GO-Au nanocomposite. The result indicated the presence of uniform spherical Au nanoparticles on the surface of the graphene oxide sheet. Au nanoparticle size varies from 6 to 10 nm without agglomeration.

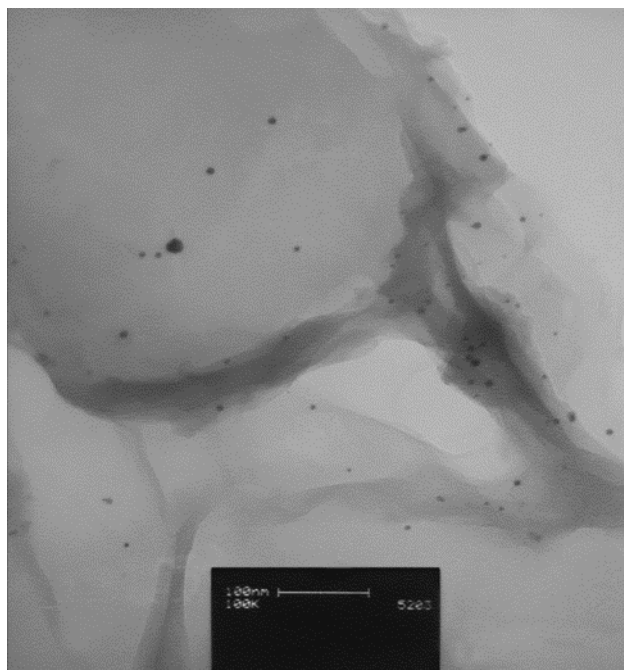


**Figure 3.** TEM image of GO-Au nanocomposite.

### 3.2. Adsorption dosage.

Dye removal by using different amounts of GO-Au nanocomposite is shown in Figure 4. Adsorbent samples (15 and 30 mg) were added to a beaker containing 10 mL of 10 mg/L MO and MB solution. Increasing the amount of nanocomposite to 30 mg increases the adsorption process. In the first 15 minutes, complete absorption and balance are established.

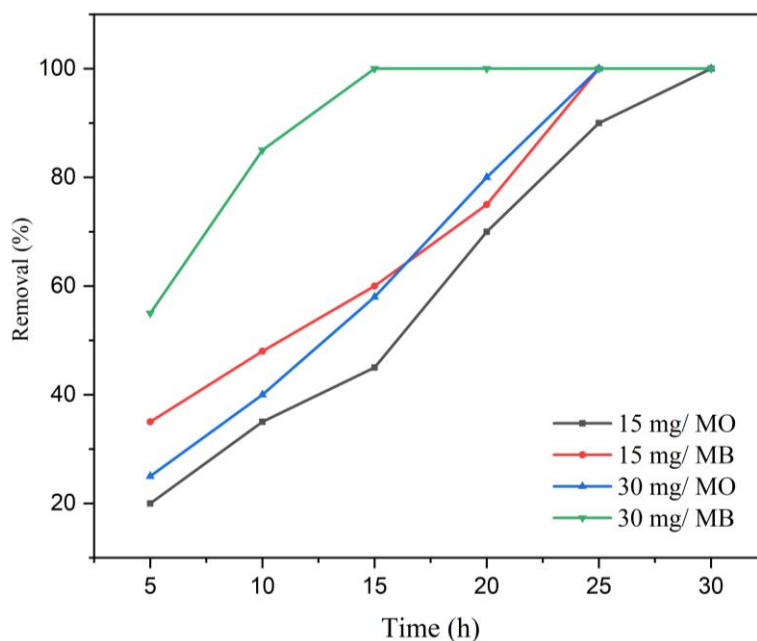


**Figure 4.** Effect of the amount of adsorbent of adsorption GO-Au nanocomposite.

#### 3.2.1. Kinetics study of dye removal.

Kinetic parameters help predict the model and adsorption rate. Both pseudo-first-order [26] and pseudo-second-order models were used for this study to understand adsorption mechanisms and kinetics.

Pseudo-first order model:

$$\log(q_e - q_t) = \log q_e - \frac{k_1}{2.303} t \quad (3)$$

Pseudo-second order model:

$$\frac{t}{q_t} = \frac{1}{k_2(q_e)^2} + \frac{t}{q_e} \quad (4)$$

where,  $q_e$  and  $q_t$  are the amount of adsorbed MO and MB ( $\text{mg g}^{-1}$ ) at equilibrium and at time  $t$  (min), correspondingly. Moreover,  $k_1$  shows the rate constant of pseudo-first-order reaction ( $\text{min}^{-1}$ ),  $h$  is the initial rate constant and  $k_2$  represents the rate constant of the pseudo-second-order reaction ( $\text{g mg}^{-1} \text{min}^{-1}$ ).

Figure 5 (A) and (B) show the straight-line plots of  $t/q_t$  vs.  $t$  and  $\log(q_e - q_t)$  vs.  $t$  for different primary dye concentrations for the pseudo-second-order kinetic model and first-order kinetic model. Table 1 shows the absorption rate constants. The correlation coefficient ( $R^2$ ), and the experimental and calculated data are used to study the model's validity. As expected for MO and MB adsorption on GO-Au nanocomposite, the second-order kinetic model has better prediction than a first-order kinetic model, with correlation coefficients  $R^2 = 0.9917$  and  $R^2 = 0.9865$ , respectively.

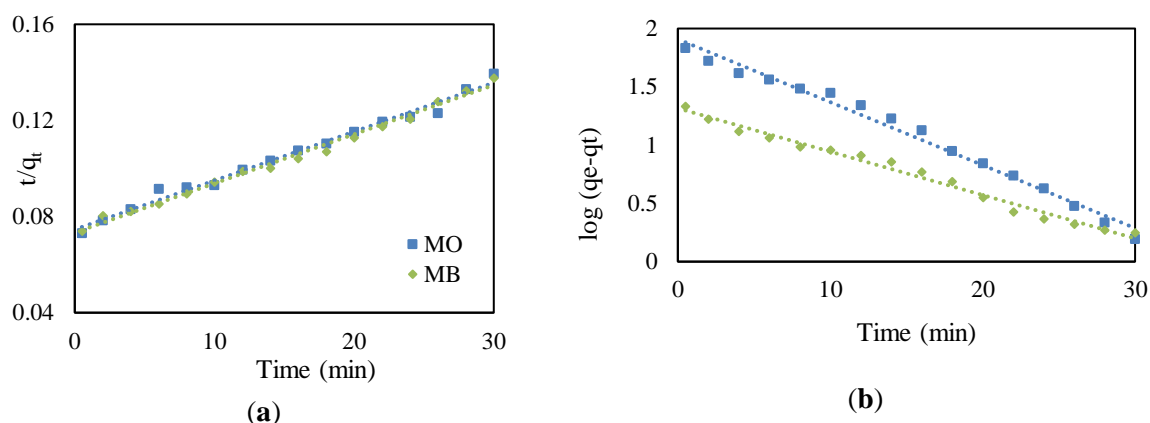


**Figure 5.** Plots of  $t/q_t$  vs.  $t$  (A) and  $\log(q_e - q_t)$  vs.  $t$  (B) for MO adsorption by GO-Au nanocomposite.

**Table 1.** Kinetics constants for dye adsorption.

Dye	Pseudo-first-order			Pseudo-second-order		
	$K_1, \text{min}^{-1}$	$q_e, \text{mg/g}$	$R^2$	$K_2, \text{g/(mg.min)}$	$q_e, \text{mg/g}$	$R^2$
MB	0.5246	15.46	0.9829	0.1769	19.72	0.9917
MO	0.4756	13.54	0.9778	0.1612	20.25	0.9865

### 3.2.2. Adsorption isotherms.

Adsorption isotherms are elementary necessities for the design of adsorption systems intended for the removal of pollutants. Different isotherms, such as Langmuir and Freundlich models, were tried [27,28]. The adsorption isotherms of Langmuir (Equation 5) and Freundlich (Equation 6) are usually used to study the adsorption activity.

Langmuir equation can be written here:

$$\frac{C_e}{q_e} = \frac{1}{K_L Q_0} + \frac{C_e}{Q_0} \quad (5)$$

where  $C_e$ ,  $K_L$  and  $Q_0$  are the equilibrium concentration of dye solution ( $\text{mg/L}$ ), Langmuir constant ( $\text{L/mg}$ ), and the maximum adsorption ability ( $\text{mg/g}$ ), respectively.

The Freundlich isotherm can be explained by:

$$\log q_e = \log K_F + \frac{\log C_e}{n} \quad (6)$$

where  $K_F$  is the adsorption ability at a unit concentration ( $\text{L/g}$ ), and  $1/n$  is the adsorption intensity.



Based on the Langmuir and the Freundlich isotherms for dye adsorption, linear plots of  $C_e/q_e$  against  $C_e$  and  $\log q_e$  vs.  $\log C_e$  are designed. The values of  $Q_0$ ,  $K_L$ ,  $K_F$ ,  $n$ , and  $R^2$  are shown in Table 2.

**Table 2.** Linearized isotherm coefficients for dye adsorption.

Dye	Langmuir isotherm			Freundlich isotherm		
	$Q_0$	$K_L$	$R^2$	$K_F$	$n$	$R^2$
MB	52.754	0.016	0.720	16.136	0.993	0.997
MO	13.330	0.371	0.742	8.100	0.500	0.985

### 3.2.3. Regeneration/desorption of adsorbent.

Figure 6 is shown the reusability of GO-Au nanocomposite for MO and MB adsorption. The nanocomposite was recycled three times in comparable situations. Before each step, the adsorbent was collected with an external magnet, washed with ethanol, and deionized water multiple times to eliminate the adsorbed, dried, and reused species. The results showed a slight decrease in discoloration efficiency, revealing the consistent behavior of these products for the adsorption cycles added for water treatment.

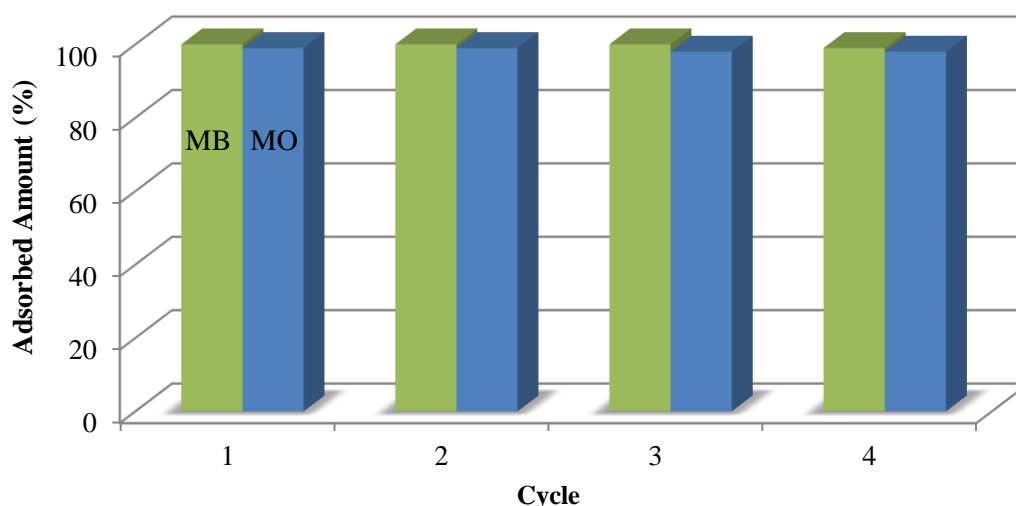


**Figure 6.** Regeneration and reusability of GO-Au nanocomposite.

## 4. Conclusions

We successfully produced GO-Au nanocomposite with a significant surface area by an easy method. The study of the resulting products' adsorption efficiency showed a good nanocomposite adsorption capability compared with zinc ferrite nanoparticles for water treatment. Both magnetic characteristics for recovery and proper surface area can nominate the produced nanocomposite as a great adsorbent for water purification.

## Funding

This research received no external funding.

## Acknowledgments

This work was supported by the Zanjan University of Medical Sciences and the University of Zanjan.

## Conflicts of Interest

The authors declare no conflict of interest.

## References

1. Tara, N.; Siddiqui, S.I.; Rathi, G.; Chaudhry, S.A.; Asiri, A.M. Nano-engineered Adsorbent for the removal of dyes from water: A review. *Current Analytical Chemistry* **2020**, *16*, 14–40, <https://doi.org/10.2174/1573411015666190117124344>.
2. Sajid, M.; Nazal, M.K.; Baig, N.; Osman, A.M. Removal of heavy metals and organic pollutants from water using dendritic polymers based adsorbents: a critical review. *Separation and Purification Technology* **2018**, *191*, 400–423, <https://doi.org/10.1016/j.seppur.2017.09.011>.
3. Velusamy, S.; Roy, A.; Sundaram, S.; Kumar Mallick, T. A review on heavy metal ions and containing dyes removal through graphene oxide-based adsorption strategies for textile wastewater treatment. *The Chemical Record* **2021**, *21*, 1570–1610, <https://doi.org/10.1002/tcr.202000153>.
4. Januário, E.F.D.; Vidovix, T.B.; Beluci, N.d.C.L.; Paixão, R.M.; da Silva, L.H.B.R.; Homem, N.C.; Bergamasco, R.; Vieira, A.M.S. Advanced graphene oxide-based membranes as a potential alternative for dyes removal: A review. *Science of The Total Environment* **2021**, *789*, 147957, <https://doi.org/10.1016/j.scitotenv.2021.147957>.
5. Saleem, H.; Zaidi, S.J.; Ismail, A.F.; Goh, P.S. Advances of nanomaterials for air pollution remediation and their impacts on the environment. *Chemosphere* **2022**, *287*, 132083, <https://doi.org/10.1016/j.chemosphere.2021.132083>.
6. Sadighian, S.; Abbasi, M.; Arjmandi, S.; Karami, H. Dye removal from water by zinc ferrite-graphene oxide nanocomposite. *Progress in Color, Colorants and Coatings* **2018**, *11*, 85–92, <https://doi.org/10.30509/PCCC.2018.75743>.
7. Naeem, H.; Ajmal, M.; Muntha, S.; Ambreen, J.; Siddiq, M. Synthesis and characterization of graphene oxide sheets integrated with gold nanoparticles and their applications to adsorptive removal and catalytic reduction of water contaminants. *RSC advances* **2018**, *8*, 3599–3610, <https://doi.org/10.1039/C7RA12030C>.
8. Palani, G.; Arputhalatha, A.; Kannan, K.; Lakkaboyana, S.K.; Hanafiah, M.M.; Kumar, V.; Marella, R.K. Current trends in the application of nanomaterials for the removal of pollutants from industrial wastewater treatment—a review. *Molecules* **2021**, *26*, 2799, <https://doi.org/10.3390/molecules26092799>.
9. Kennes, C.; Rene, E.R.; Veiga, M.C. Bioprocesses for air pollution control. *Journal of Chemical Technology & Biotechnology* **2009**, *84*, 1419–1436, <https://doi.org/10.1002/jctb.2216>.
10. Xue, W.; Du, J.; Li, Q.; Wang, Y.; Lu, Y.; Fan, J.; Yu, S.; Yang, Y. Preparation, Properties, and Application of Graphene-Based Materials in Tissue Engineering Scaffolds. *Tissue Engineering Part B: Reviews* **2022**, <https://doi.org/10.1089/ten.teb.2021.0127>.
11. Meng, L.; Zhang, X.; Tang, Y.; Su, K.; Kong, J. Hierarchically porous silicon–carbon–nitrogen hybrid materials towards highly efficient and selective adsorption of organic dyes. *Scientific reports* **2015**, *5*, 1–16, <https://doi.org/10.1038/srep07910>.
12. Yu, W.; Gong, K.; Li, Y.; Ding, B.; Li, L.; Xu, Y.; Wang, R.; Li, L.; Zhang, G.; Lin, S. Flexible 2D Materials beyond Graphene: Synthesis, Properties, and Applications. *Small* **2022**, *18*, 2105383, <https://doi.org/10.1002/sml.202105383>.
13. Chen, D.; Feng, H.; Li, J. Graphene oxide: preparation, functionalization, and electrochemical applications. *Chemical reviews* **2012**, *112*, 6027–6053, <https://doi.org/10.1021/cr300115g>.
14. Jian, M.; Zhang, Y.; Liu, Z. Graphene fibers: Preparation, properties, and applications. *Acta Phys. Chim. Sin.* **2022**, *38*, 2007093, <https://doi.org/10.3866/PKU.WHXB202007093>.
15. Kar, P.; Sardar, S.; Liu, B.; Sreemany, M.; Lemmens, P.; Ghosh, S.; Pal, S.K. Facile synthesis of reduced graphene oxide–gold nanohybrid for potential use in industrial wastewater treatment. *Science and Technology of advanced Materials* **2016**, *17*, 375–386, <https://doi.org/10.1080/14686996.2016.1201413>.
16. Travlou, N.A.; Kyzas, G.Z.; Lazaridis, N.K.; Deliyanni, E.A. Graphite oxide/chitosan composite for reactive dye removal. *Chemical engineering journal* **2013**, *217*, 256–265, <https://doi.org/10.1016/j.cej.2012.12.008>.
17. Nesakumar, N.; Srinivasan, S.; Alwarappan, S. Graphene quantum dots: synthesis, properties, and applications to the development of optical and electrochemical sensors for chemical sensing. *Microchimica Acta* **2022**, *189*, 1–36, <https://doi.org/10.1007/s00604-022-05353-y>.
18. Xu, Y.; Zhao, L.; Bai, H.; Hong, W.; Li, C.; Shi, G. Chemically converted graphene induced molecular flattening of 5, 10, 15, 20-tetrakis (1-methyl-4-pyridinio) porphyrin and its application for optical detection of cadmium (II) ions. *Journal of the American Chemical Society* **2009**, *131*, 13490–13497, <https://doi.org/10.1021/ja905032g>.
19. Karami, A.; Shomal, R.; Sabouni, R.; Al-Sayah, M.H.; Aidan, A. Parametric Study of Methyl Orange Removal Using Metal–Organic Frameworks Based on Factorial Experimental Design Analysis. *Energies* **2022**, *15*, 4642, <https://doi.org/10.3390/en15134642>.



20. Gao, L.; Gao, T.; Zhang, Y.; Hu, T. A bifunctional 3D porous Zn-MOF: Fluorescence recognition of Fe<sup>3+</sup> and adsorption of congo red/methyl orange dyes in aqueous medium. *Dyes and Pigments* **2022**, *197*, 109945, <https://doi.org/10.1016/j.dyepig.2021.109945>.
21. Sazezi, A.S.; Kermanian, M.; Ramazani, A.; Sadighian, S. Synthesis of Graphene Oxide/Iron Oxide/Au Nanocomposite for Quercetin Delivery. *Journal of Inorganic and Organometallic Polymers and Materials* **2022**, *32*, 1541-1550, <https://doi.org/10.1007/s10904-022-02259-3>.
22. Sontakke, A.D.; Purkait, M.K. A brief review on graphene oxide nanoscrolls: structure, synthesis, characterization and scope of applications. *Chemical Engineering Journal* **2021**, *420*, 129914, <https://doi.org/10.1016/j.cej.2021.129914>.
23. Ramazani, A.; Abrvash, M.; Sadighian, S.; Rostamizadeh, K.; Fathi, M. Preparation and characterization of curcumin loaded gold/graphene oxide nanocomposite for potential breast cancer therapy. *Research on Chemical Intermediates* **2018**, *44*, 7891-7904, <https://doi.org/https://doi.org/10.1007/s11164-018-3593-8>.
24. Misran, E.; Bani, O.; Situmeang, E.M.; Purba, A.S. Banana stem based activated carbon as a low-cost adsorbent for methylene blue removal: Isotherm, kinetics, and reusability. *Alexandria Engineering Journal* **2022**, *61*, 1946-1955, <https://doi.org/10.1016/j.aej.2021.07.022>.
25. Olorunkosebi, A.A.; Eleruja, M.A.; Adedeji, A.V.; Olofinjana, B.; Fasakin, O.; Omotoso, E.; Oyedotun, K.O.; Ajayi, E.O.B.; Manyala, N. Optimization of graphene oxide through various Hummers' methods and comparative reduction using green approach. *Diamond and Related Materials* **2021**, *117*, 108456, <https://doi.org/10.1016/j.diamond.2021.108456>.
26. Hosseini, F.; Sadighian, S.; Hosseini-Monfared, H.; Mahmoodi, N.M. Dye removal and kinetics of adsorption by magnetic chitosan nanoparticles. *Desalination and Water Treatment* **2016**, *57*, 24378-24386, doi:10.1080/19443994.2016.1143879, <https://doi.org/10.1080/19443994.2016.1143879>.
27. Özcan, A.; Öncü, E.M.; Özcan, A.S. Kinetics, isotherm and thermodynamic studies of adsorption of Acid Blue 193 from aqueous solutions onto natural sepiolite. *Colloids and Surfaces A: Physicochemical and Engineering Aspects* **2006**, *277*, 90-97, <https://doi.org/10.1016/j.colsurfa.2005.11.017>.
28. Kaykhani, M.; Hasheminasab, S.S.; Hashemi, S.H.; Sasani, M. Evaluation of Langmuir and Freundlich Isotherms for Removal of Cephalexin and Tetracycline Antibiotics By Sistan Sand from Water and Wastewater Samples. *Biquarterly Iranian Journal of Analytical Chemistry* **2021**, *8*, 32-39, <https://doi.org/10.30473/IJAC.2022.62515.1216>.